Vertical mixing induced by tidally generated internal waves in the Kuril Straits

Tomohiro NAKAMURA[1], Toshiyuki Awaji[1], Takaki Hatayama[1], Kazunori Akitomo[1], Takatoshi Takizawa[2] and Masao Fukasawa[3]

[1] Department of Geophysics, Kyoto University, Kyoto, Japan

[2] Japan Marine Science and Technology Center, Yokosuka, Japan

[3] School of Marine Science and Technology, Tokai University, Shizuoka, Japan

Abstract. Numerical experiments are performed to investigate the vertical mixing induced by tidally generated internal waves in the Kuril Straits. The results show that in contrast to previous theories, intense short internal waves generated at the sill breaks by the subinertial K_1 current can propagate upstream as the tidal current slackens. Our theoretical considerations identify these short waves as unsteady lee waves, which tend to be trapped at the generation region and grow into large-amplitude waves. Superposition of a propagating unsteady lee wave and a newly generated lee wave over a sill causes significant wave breaking leading to a maximum vertical diffusivity of $\sim 10^3$ cm^2 s^{-1}. This quite intense mixing reaches down to the density layer of the NPIW, thus suggesting that lee waves generated by interactions between the K_1 current and the bottom topography of the Kuril Straits play an important role in the formation of the NPIW.

Introduction

Recent observations (e.g., Kawasaki and Kono, 1994) show the presence of strong vertical mixing in the Kuril Straits, implying that such strong vertical mixing is one of the major factors in supplying low salinity water required for the production of the NPIW (Talley, 1991). Several studies suggested that tidal mixing is responsible for this intense vertical mixing. However, the actual physical mechanisms are still unknown. According to observations, the currents are dominated by the diurnal tidal components in the Kuril Straits, and the semidiurnal components are rather weak. Swift K_1 currents have been thought to cause intense vertical mixing by interactions with large-amplitude sills in the Kuril Straits. However, this situation is out of the range of previous theories for the growth of oceanic internal waves, which assume that an oscillating tidal flow over an obstacle excites only internal waves at its tidal frequency (internal tides). Since the diurnal tides are subinertial around this high latitude ($\sim 47°$ N), internal tides at the K_1 tidal frequency are not freely propagating waves. This fact prevents us from using the previous theoretical models. For example, Hibiya's (1986) theory assumes that internal tides propagating upstream are trapped at the generation region and amplified when the barotropic flow is critical (i.e., when the Froude number F_n is unity where F_n is the ratio of the barotropic tidal flow speed to phase speed of nth mode). Thus, as a first step toward clarifying the physics responsible for the vertical mixing in the Kuril Straits, we have performed numerical simulations of tidally generated internal waves and have estimated the vertical mixing induced by those waves.

Numerical model

The model bottom topography is representative of the sills in the northeastern part of the Kuril Straits, where tidal currents are so strong that they can cause considerable mixing (Fig. 1). In order to simulate vertical mixing by internal waves, we used a vertically two-dimensional nonhydrostatic f-plane model with horizontal and vertical grid sizes of 500 m and 10 m, respectively. The horizontal and vertical eddy viscosity coefficients are assigned the relatively small values of 2×10^5 cm^2 s^{-1} and 0.1 cm^2 s^{-1}, respectively, so that their effect on mixing is small enough to demonstrate the wave mixing clearly. As basic forcing terms for internal wave generation, barotropic K_1 and M_2 currents are given at both lateral boundaries. Their maximum speeds at the sill top are 0.5 m s^{-1} for the K_1 case and 0.2 m s^{-1} for the M_2 case, as determined from our preceding barotropic tidal simulations (Awaji et al., 1999). We took account of the effect of rotation to distinguish the physics of waves generated by the subinertial K_1 flow from that of the superinertial M_2

flow in the Kuril Straits. At the bottom boundary, a no-slip condition is imposed in the sill region and a free-slip condition is imposed in the deep region with the flat bottom. A rigid-lid approximation is used at the surface to restrict our attention to internal processes. The initial vertical profiles of potential temperature and salinity are from the summertime climatology in the Kuril Basin of the Okhotsk Sea (not shown). With these vertical profiles, model calculations start at the beginning of rightward flow so that wave generation processes can be seen clearly.

Model results

Figure 2 shows the map of the internal mode stream function defined by Lamb (1994) during the second cycle in the M_2 case. As past studies show, first-mode internal waves are generated on the slopes of the sill (Fig. 2a), and propagate away from the sill. Wave generation on the sill slopes by rightward flow continues for up to 1.5 periods when the flow stops (Fig. 2b), and the generated waves propagate away from the sill after 1.75 periods. In the half period of leftward flow (Figs. 2c and d), almost the same sequence of events can be observed, but with their phase reversed. The linear dispersion relation gives the frequency of first-mode waves of 1.4×10^{-4} s^{-1}, almost equal to the M_2 frequency. Thus the first mode waves seen in Figure 2 can be identified as typical internal tides at the M_2 frequency. Since most of internal mode energy generated by the M_2 flow propagates away as first-mode internal tides, large-amplitude internal waves are not formed and breaking is absent in the M_2 case. Consequently, vertical mixing induced by waves generated by the M_2 flow is probably not strong enough to cause significant freshening in the Kuril Straits. The time series of the internal mode stream function in the K_1 case (Fig. 3) shows quite different behavior from that of the M_2 case primarily because the Kuril Straits are located over the critical latitude for the K_1 tide. For example, sill-scale cells do not propagate away, and, in contrast to the M_2 case, intense disturbances exist on small scales. We direct our attention to intense smaller-scale disturbances detected in Figure 3. These short waves may cause considerable mixing because shorter wavelengths induce stronger dissipation and so release energy for mixing, and because the process of wave breaking takes place at smaller amplitudes for waves of shorter wavelength. Figure 3 clearly shows the movement of small-scale disturbances labelled as A_1, B_1, A_2, B_2, a_1, and b_1 from left to right, with the tidal period during which they are produced indicated by subscripts and with the direction of the tidal flow at the time of their production indicated by capital (rightward) and small (leftward) letters. The propagation speeds of these small-scale disturbances estimated from Figure 3 ($0.3 \sim 1.4$ m s^{-1}) are different from the tidal flow speed (less than 0.125 m s^{-1}). This fact means that they are freely-propagating internal waves. Thus,

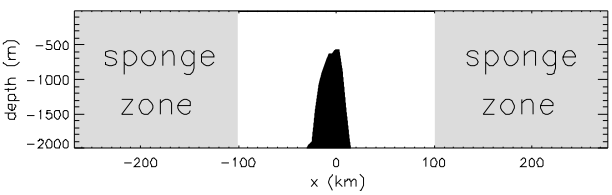

Fig. 1 The model topography, representing the vertical cross-section of a strait in the northeastern part of the Kuril Islands, where tidal currents are strong enough to cause considerable mixing.

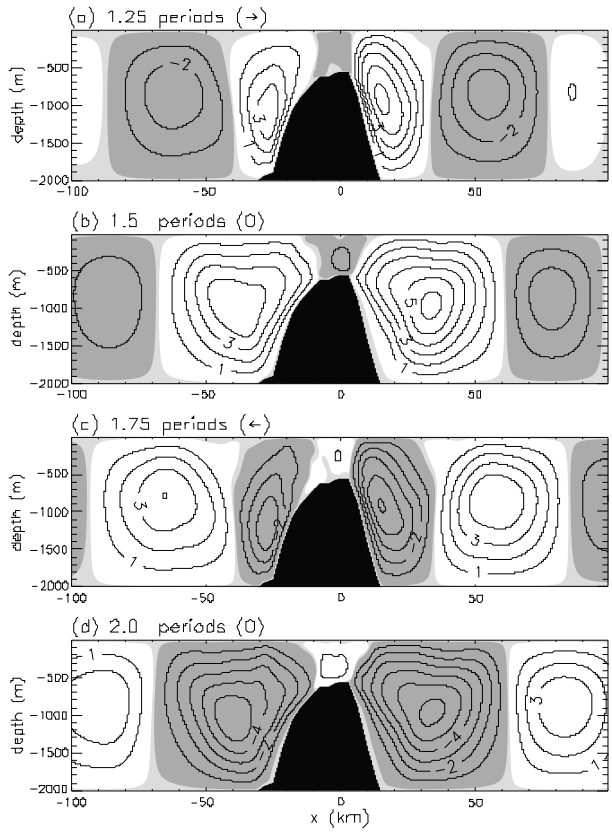

Fig. 2 The time series of the internal mode stream function in the M_2 case during the second tidal period; after (a) 1.25, (b) 1.5, (c) 1.75, and (d) 2.0 periods. The contour interval is 1.0×10^5 cm^2 s^{-1}. Values in unshaded areas and the darkly shaded areas are positive and negative, respectively, and the absolute values in the lightly shaded areas are less than 1×10^4 cm^2 s^{-1}.

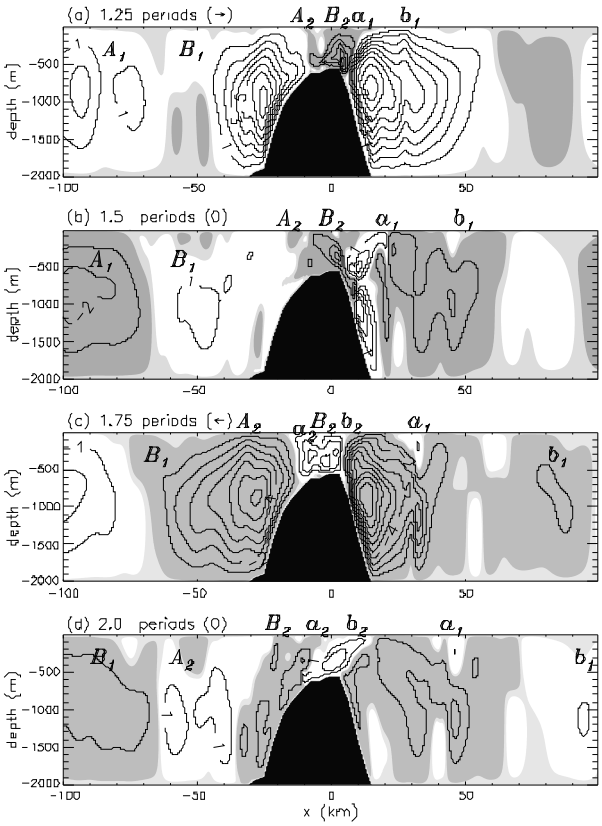

Fig. 3 Same as in Figure 2 but for the K_1 case.

their frequencies must be larger than the inertial frequency, despite the fact that the K_1 frequency is subinertial. Therefore, previous theoretical models cannot explain the generation of such intense short waves as described earlier. Furthermore, these features are produced by rightward (leftward) flow and propagate leftward (rightward), indicating that they move only in the upstream direction as determined at their generation time. This is also inconsistent with the character of internal tides which propagate in both directions. From these considerations, it is inferred that the intense short waves in our model must represent another class of wave, and thus we reinvestigate the excitation mechanism of internal waves by a tidal flow in the next section.

The excitation mechanism of unsteady lee waves

To investigate the wave excitation properly, it is necessary to consider the total time variation of the forcing to which fluid parcels are subjected. Representing the forcing as F, the total time variation of the forcing DF/Dt is given in Eulerian variables as,

$$\frac{DF}{Dt} = \frac{\partial F}{\partial t} + U_i \frac{\partial F}{\partial x_i}, \qquad (1)$$

where U_i represents the velocity of the basic flow in the x_i direction. Most of the previous theories of internal waves generated by an oscillating tidal flow have neglected the advection effect (the second term) in wave excitation. However, Eq. (1) shows that in regions where the tidal flow is strong and the horizontal scale of forcing is small, such as sill tops or shelf breaks, wave excitation cannot be fully comprehended unless the advection effect on wave excitation is incorporated. To easily specify the nature and structure of tidally generated internal waves, our discussion is restricted to the vertically two-dimensional case ($\partial/\partial y = 0$), and we assume that the flow varies as a single harmonic component of frequency σ_f in time. Then, the vertical velocity W at the bottom is given by

$$W = W(x,t) = e^{i\sigma_f t} \int_{-\infty}^{\infty} \hat{W}_0(k) e^{-ikx}\, dk, \qquad (2)$$

using a Fourier transformation. We can describe the wave forcing (2) in the neighborhood of $x = x_0$ and $t = t_0$ in the moving frame X. After some manipulation, the vertical velocity W splits into the sum of traveling waves propagating with two different phase velocities as

$$\begin{aligned} &W(x,t) \\ &= \int_0^{\infty} \hat{W}_0(k) e^{i\sigma_f t_0} \{\exp[-i(kX + (kU(x_0,t_0) + \sigma_f)\tau)] \\ &\quad - \exp[+i(kX + (kU(x_0,t_0) - \sigma_f)\tau)]\}\, dk. \qquad (3) \end{aligned}$$

This expression shows that the internal wave excited in the neighborhood of $x = x_0$ and $t = t_0$ by the basic flow (U, W) is composed of a sum of monochromatic waves with frequency of $-kU(x_0,t_0) \pm \sigma_f$ and horizontal wavenumber of k. Thus, according to the nondimensional parameter kU_0/σ_f, we can classify internal waves excited by an oscillating flow into unsteady lee waves (when $kU_0/\sigma_f \gg 1$) and "mixed tidal lee waves" (when $kU_0/\sigma_f \sim 1$), in addition to internal tides (when $kU_0/\sigma_f \ll 1$) which previous theoretical models have considered. These three types of "topographic internal waves" have the following properties: Unsteady lee waves have the frequencies of $-kU(t)$, and their phase velocities are $-U(t)$. Thus, unsteady lee waves can propagate in the upstream direction at their excitation time. The amplitudes of unsteady lee waves depend on the magnitude of the forcing at the time of their excitation, so that the waves generated around the time of maximum flow have maximum amplitudes. Such

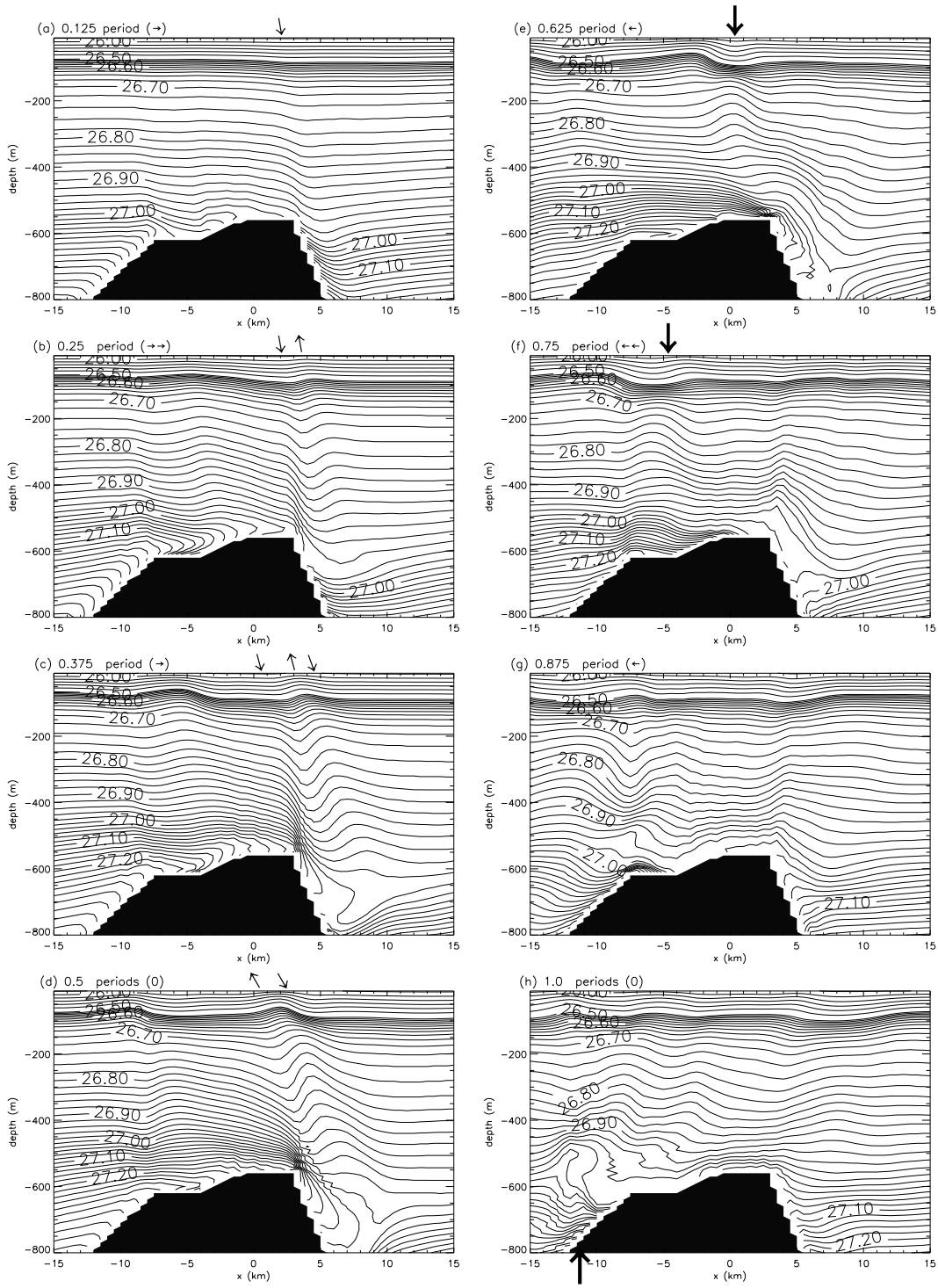

Fig. 4 The evolution of potential density (σ_θ) around the sill top in the K_1 case, during the first period, after (a) 0.125, (b) 0.25, (c) 0.375, (d) 0.5, (e) 0.625, (f) 0.75, (g) 0.875, (h) 1 period, when the generation process of the large-amplitude unsteady lee wave can be clearly seen. For $\sigma_\theta < 26.5$, the contour interval is 0.1 σ_θ. For $\sigma_\theta \geq 26.5$ the contour interval is 0.02 σ_θ.

unsteady lee waves are excited in a region where the curvature of topography is sufficiently large, such as shelf breaks. In contrast, internal tides have a frequency of σ_f and a constant phase velocity of $\pm\sigma_f/k$, and propagate in both directions, as shown in previous studies. In the intermediate range, excited waves have intermediate properties between those of lee waves and internal tides, and we name such waves "mixed tidal lee waves". Consideration of the frequency of these new waves allows us to explain the reason why the subinertial K_1 flow can generate freely-propagating internal waves at the sill top. The co-phase lines of the internal wave generated at the break (not shown) extend only in one direction, consistent with the character of unsteady lee waves. Thus, we conclude that the intense short waves simulated in the K_1 case are unsteady lee waves.

The evolution of large-amplitude unsteady lee waves

Figure 4 shows the evolution of potential density (σ_θ) in the K_1 case up to 1 period, where the generation process of the intense short waves can be seen clearly. As expected from our theoretical model, small-scale vertical velocity distributions produced at sudden changes in the sill slope generate a relatively large depression of small horizontal length at the right-hand break and adjacent weak elevation and depression over the left-hand break and sill top. The displacement at the right-hand break continues to grow until the end of the rightward flow to form a large-amplitude ($\sim$ 100 m) unsteady lee wave (Fig. 4d). As the rightward flow vanishes after 0.5 period, the large-amplitude unsteady lee wave begins to propagate in the upstream direction at the generation time (leftward). When propagating across the sill, this large-amplitude wave encounters an unsteady lee wave newly generated at the left-hand break by the leftward flow. These lee waves are superposed and interact with each other (after 0.875 period). As the flow turns to the right, the large-amplitude elevation at the foot of the lee wave gradually breaks, propagating rightward, and causes vigorous vertical mixing over the sill top. In this way, large-amplitude unsteady lee waves induce intense vertical mixing, and relatively vertically uniform water is produced over and around the sill top in the K_1 case as seen in Figure 5a. The feature of this map has good similarities with that of observations (Fig. 5b), supporting our model's realism.

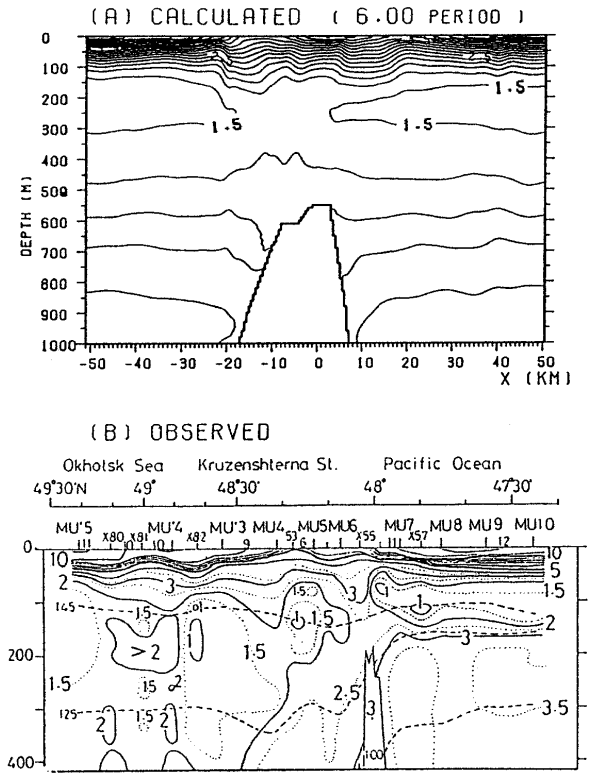

Fig. 5 (a) The calculated potential temperature distribution after 6 periods, and (b) the observed potential temperature distribution in the Kruzenshterna Strait.

Vertical mixing induced by internal waves

Here, we estimate the intensity of the resulting vertical mixing in terms of diffusivity. To relate the result to the parameterizations used in general circulation models, we estimate the vertical diffusivity K_z^E from an Eulerian point of view with the following Fickian formulation,

$$K_z^E = \left| \frac{\overline{S'w'}}{dS_0/dz} \right| \tag{4}$$

where dS_0/dz is the vertical gradient of the initial salinity profile, and $\overline{S'w'}$ is salinity flux induced by perturbations, averaged over one tidal period. In the M_2 case, the estimated diffusivity using the calculated velocity fields in the second period is not so large ($\sim$ 10 cm^2 s^{-1}), as expected earlier. In contrast, the value in the K_1 case is very large around the sill ($\sim 10^3$ cm^2 s^{-1}) and relatively small in other regions. This is mainly due to large-amplitude unsteady lee waves propagating over the sill and their superposition on unsteady lee waves newly generated by

the reversed flow leading to significant wave breaking.

Summary

In order to clarify the role played by intense vertical mixing in the Kuril Straits on the modification of water properties, we numerically investigated internal waves generated through the interaction between the tidal currents and the sill and their effect on mixing, using a nonhydrostatic f-plane model. The model results reveal the following. Internal waves at the tidal frequency (internal tides) generated by the K_1 flow are trapped to the sill, because the K_1 tide is subinertial in the Kuril Straits. Since the strong barotropic flow is further intensified near the bottom by the trapped internal tides, large-amplitude free-propagating internal waves of short wavelengths are repeatedly generated and break around the sill top, thus producing relatively vertically uniform water over and around the sill top. On the other hand, in the M_2 case, since most of the generated internal waves propagate away as first-mode internal tides, their amplitudes do not become so large. As a result, the M_2 tidal current does not have the potential to cause significant vertical mixing to explain the freshening in the Kuril Straits. Our theoretical consideration identifies the large-amplitude short waves in the K_1 case as unsteady lee waves, whose existence has been neglected in previous oceanic internal wave theories. Interestingly, the superposition of a propagating unsteady lee wave and a newly generated lee wave over the sill generates a large-amplitude internal wave, which causes wave breaking and induces intense vertical mixing over the sill top.

References

Awaji, T., Nakamura, T. Hatayama, T. and Akimoto, K. 1999. Tidal exchange through the Kuril Straits. pp. 77–82. In *Proc. Second Workshop on the Okhotsk Sea and Adjacent Areas, PICES Sci. Rep. No. 12*, Labonov, V.B., Nagata, Y. and Riser, S.C. (eds.), Sidney, B.C., Canada.

Hibiya, T. 1986. Generation mechanism of internal waves by tidal flow over a sill. *J. Geophys. Res., 91*, 7696–7708.

Kawasaki, Y. and Kono, T. 1994. Distribution and transport of subarctic waters around the middle of Kuril Islands. *Sea and Sky, 70*, 71–84. (in Japanese)

Lamb, K.G. 1994. Numerical experiments of internal wave generation by strong tidal flow across a finite amplitude bank edge. *J. Geophys. Res., 99*, 843–864.

Talley, L.D. 1991. An Okhotsk Sea water anomaly: Implications for ventilation in the North Pacific. *Deep-Sea Res., 38*(Suppl. 1), S171–190.

Talley, L.D. 1993. Distribution and formation of North Pacific Intermediate Water. *J. Phys. Oceanogr., 23*, 517–537.